25.8 W All-Fiber Mid-Infrared Supercontinuum Light Sources Based on Fluorotellurite Fibers

Xiaohui Guo, Zhixu Jia, Yadong Jiao, Zhenrui Li, Chanfei Yao, Minglie Hu, Yasutake Ohishi, *Member, IEEE*, Weiping Qin, and Guanshi Qin

***Abstract*— In this letter, we demonstrate a 25.8 W all-fiber mid-infrared supercontinuum (SC) light source based on fluorotellurite fibers. All-solid fluorotellurite fibers are fabricated by using a rod-in-tube method. A 56 cm long fluorotellurite fiber with a core diameter of ∼11 μm is used as the nonlinear medium and a high power 1.93∼2.5 μm SC fiber laser as the pump source. The fluorotellurite fiber is connected to the output silica fiber of the pump source by direct fusion splicing, leading to the formation of the compact all-fiber structure. For a pump power of ∼42.6 W, we obtain a 25.8 W SC light source with a spectral range from 0.93 to 3.99 μm. The corresponding optical-to-optical conversion efficiency is about 60.6%. To the best of our knowledge, this is the first time to report all-fiber high power mid-infrared SC light source based on fluorotellurite fibers. Our results pave the way to apply mid-infrared SC light sources based on fluorotellurite fibers for real applications.**

***Index Terms*— All-fiber configuration, direct fusion splicing, high power mid-infrared supercontinuum light source, fluorotellurite fibers.**

I. Introduction

MID-INFRARED supercontinuum (MIR-SC) light sources have attracted much attention due to their numerous applications in frequency metrology, molecular spectroscopy, biomedicine, real-time high-resolution optical coherence tomography, hyper-spectral microscopy, long-distance remote sensing, defense, and security [1]–[5]. The brightness of MIR-SC light sources has been shown to be orders of magnitude higher than that of synchrotrons [4]. Recently, many efforts have been made to construct all-fiber high power MIR-SC light sources for satisfying the requirements of various applications. Several types of soft-glass fibers (including fluoride, fluorotellurite fibers) have been developed for constructing all-fiber high power (>10 W) MIR-SC light sources. For $53ZrF_4$-$20BaF_2$-$4LaF_3$-$3AlF_3$-20NaF (ZBLAN) fibers, in 2009, Xia *et al.* reported an all-fiber SC light source with an average power of ∼10.5 W and a continuous spectrum from 0.8 to 4 μm, in which the ZBLAN fiber was connected to the output silica fiber of the pump source by a butt-coupling method [6]. In 2014, Yang *et al.* demonstrated a 13 W all-fiber MIR-SC light source with a spectral range from 1.9 to 4.3 μm in which a 2 μm master oscillator power amplifier system was used as the pump source and the ZBLAN fiber was mechanically spliced to the output silica fiber of the pump source [7]. Liu *et al.* reported a 21.8 W all-fiber SC generation from 1.9 to beyond 3.8 μm by connecting the ZBLAN fiber to the silica fiber via a butt-coupling method [8]. Although the butt-coupling or mechanical splicing method could be used to construct all-fiber high power MIR-SC light sources, the long-term stability of such MIR-SC light sources needed to be improved for real applications. For this purpose, the direct fusion splicing method was developed for connecting soft glass fibers to silica fibers. Based on this technique, in 2019, Yang *et al.* reported an all-fiberized 30 W SC generation from 1.9 to 3.35 μm in a piece of ZBLAN fiber [9]. Soon after that, they further extended the spectral coverage of the SC source based on ZBLAN fibers to 1.9-4.3 μm, and the obtained output power was about 20.6 W [10]. For the fluoroindate fibers, in 2019, Wu *et al.* reported an 11.3 W all-fiber MIR-SC light source with a spectral range from 0.8 to 4.7 μm, in which all-fiber structure was formed by a direct fusion splicing between the fluoroindate fiber and the silica fiber [11]. However, since ZBLAN or fluoroindate fibers have poor chemical and thermal stability, the long-term stability of high-power fluoride-fiber-based MIR light sources needs to be improved for real applications [12].

Recently, fluorotellurite fibers based on TeO_2-BaF_2-Y_2O_3 (TBY) glasses have been developed by us. Such fibers had a broadband transmission window of 0.4∼6 μm and stable chemical and thermal properties compared to fluoride and chalcogenide fibers. The transition temperature of the TBY glass was about 424 °C, which was much higher than that of previously reported tellurite, ZBLAN, fluoroindate, and chalcogenide glasses. The figure-of-merit parameter for characterizing the thermal mechanical properties of a laser material

Manuscript received August 30, 2021; revised January 31, 2022; accepted March 2, 2022. Date of publication March 10, 2022; date of current version March 24, 2022. This work was supported in part by the National Key Research and Development Program of China under Grant 2020YFB1805800; in part by the National Natural Science Foundation of China (NSFC) under Grant 61827821, Grant 62090063, Grant 62075082, Grant U20A20210, Grant 61527823, and Grant 11774132; in part by the Key Technology Research and Development Project of Jilin Province under Grant 20180201120GX; in part by the Field Funding for Equipment Pre-Research under Grant 61404140106; in part by the Opened Fund of the State Key Laboratory of Integrated Optoelectronics; and in part by the Opened Fund of State Key Laboratory of Luminescence and Applications under Grant SKLA-2019-05. *(Corresponding authors: Zhixu Jia; Guanshi Qin.)*

Xiaohui Guo, Zhixu Jia, Yadong Jiao, Zhenrui Li, Chanfei Yao, Weiping Qin, and Guanshi Qin are with the State Key Laboratory of Integrated Optoelectronics, College of Electronic Science and Engineering, Jilin University, Changchun 130012, China (e-mail: jiazx@jlu.edu.cn; qings@jlu.edu.cn).

Minglie Hu is with the Ultrafast Laser Laboratory and the Key Laboratory of Opto-Electronic Information Science and Technology, Ministry of Education, College of Precision Instruments and Opto-Electronics Engineering, Tianjin University, Tianjin 300072, China.

Yasutake Ohishi is with the Research Center for Advanced Photon Technology, Toyota Technological Institute, Nagoya 468-8511, Japan.

Color versions of one or more figures in this letter are available at https://doi.org/10.1109/LPT.2022.3158813.

Digital Object Identifier 10.1109/LPT.2022.3158813

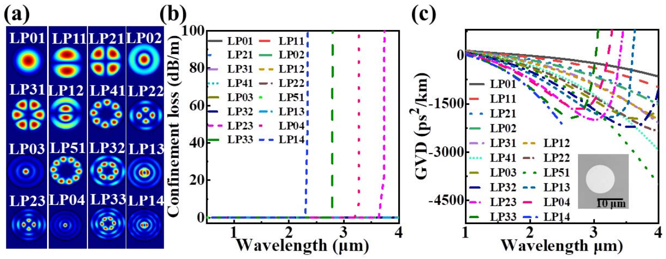

Fig. 1. Calculated (a) intensity distribution profiles, (b) confinement losses and (c) GVD profiles of LP modes (including LP01, LP11, LP21, LP02, LP31, LP12, LP41, LP22, LP03, LP51, LP32, LP13, LP23, LP04, LP33 and LP14 modes) in the fluorotellurite fiber. Inset: Scanning electron micrograph of the fluorotellurite fiber.

was also measured for TBY and ZBLAN glasses, which indicated that TBY glass fibers might bear stronger thermal shock than ZBLAN glass fibers [13]. Very recently, a 22.7 W fluorotellurite-fiber-based MIR-SC light source with a spectral range from 0.93 to 3.95 μm was demonstrated by us [14]. Whereas, the fluorotellurite fiber was connected to the output silica fiber of the pump source by using a mechanical splicing method. Despite recent progress on high power MIR-SC light sources based on fluorotellurite fibers, it is necessary to explore the ways of the realization of all-fiber high-power MIR-SC light sources based on fluorotellurite fibers and further power scaling.

In this letter, we reported a 25.8 W all-fiber MIR-SC Light source based on fluorotellurite fibers. The fluorotellurite fiber was connected to the output silica fiber of the pump source by direct fusion splicing, leading to the formation of the compact all-fiber structure. For a pump power of ~42.6 W, we obtained a 25.8 W SC laser source with the spectral range from 0.93 to 3.99 μm. The corresponding optical-to-optical conversion efficiency was about 60.6%. To the best of our knowledge, this is the first report of an all-fiber high power (over 25 W) MIR-SC light source based on fluorotellurite fibers.

II. Experiments and Results

All-solid fluorotellurite fibers were fabricated by using a rod-in-tube method. The core and cladding materials for all-solid fluorotellurite fibers have the compositions of TBY and AlF_3-CaF_2-BaF_2-SrF_2-MgF_2-YF_3-TeO_2 (ACBSMYT), respectively. The two fluorotellurite glasses have similar transmission window, similar linear thermal expansion coefficients (σ) (148.4×10^{-7}/°C for TBY glass, 153.8×10^{-7}/°C for ACBSMYT glass) and similar soften temperatures (T_s) (439 °C for TBY glass, 449 °C for ACBSMYT glass) [15]. However, the refractive index of ACBSMYT glass (1.466 at 2 μm) is much lower than that of TBY glass (1.858 at 2 μm), which makes the fabricated fluorotellurite fibers have an ultra-high NA of ~1.14 at 2 μm. The inset of Fig. 1(c) shows a scanning electron micrograph image of the fabricated all-solid fluorotellurite fiber. The fiber had a step-index structure and a core diameter of ~11 μm. The group velocity dispersion (GVD) profiles of the fiber were calculated by using commercial software MODE solutions (Lumerical Solutions, Inc.) with the full vectorial finite difference method. Figures 1(a), 1(b) and 1(c) show the calculated intensity distribution profiles, the confinement losses and GVD profiles of LP modes (including LP01, LP11, LP21, LP02, LP31, LP12, LP41, LP22, LP03, LP51, LP32, LP13, LP23, LP04, LP33 and LP14 modes) in the fluorotellurite fiber. The confinement losses of LP23, LP04, LP33 and LP14 modes become large in the wavelength range of >2500 nm, which is detrimental for generating mid-infrared SC light (>2500 nm). And with an increase of the order number, the first zero-dispersion wavelength shifted to short wavelength region and the second zero-dispersion wavelength appeared. The transmission loss at 2 μm of the fiber was measured by using a cut-back method and the measured value was about 1.7 dB/m. The nonlinear coefficients at 2 μm for those modes of the fiber were calculated to be about 22.4, 16.1, 16.4, 28.9, 16.6, 20.0, 21.6, 27.8, 32.7, 20.2, 21, 24.3, 31.3, 34.9, 22.8 and 27 $km^{-1}W^{-1}$, respectively, by using a nonlinear refractive index of 3.5×10^{-19} m^2W^{-1} for fluorotellurite glasses [14].

To construct all-fiber MIR-SC light source based on fluorotellurite fibers, direct fusion splicing was used to realize the connection between fluorotellurite fibers and silica fibers. The fusion splicer we used was a CO_2 laser fiber fusion processing workstation (Fujikura, LZM-100). The fluorotellurite fiber had a core diameter of ~11 μm and an outer (or cladding) diameter of ~200 μm. The silica fiber had a core/cladding diameter of ~10/130 μm. Since the thermal and mechanical properties of the fluorotellurite glass was different from that of silica glass, fusion splicing could not be done by using the CO_2 laser to heat the ends of fluorotellurite and silica fibers together, just like fusion splicing between silica fibers. In our experiment, first, both fluorotellurite and silica fibers were cleaned and cleaved perpendicularly by using a fiber cleaver (Fujikura, CT106). Second, the cleaved fibers were mounted on the fiber holders in the CO_2 laser fiber fusion processing workstation. Third, the fiber end gap and the overlap amount of splicing were set to be 1 and 5 μm, respectively. The heater was located at the side of fluorotellurite fiber. As the increase of the power of the CO_2 laser, the temperature at the cleaved end increased and exceeded the T_g of the fluorotellurite fiber, then, the two fibers were pushed toward each other immediately and fused together. Finally, the temperature around the fusion splicing point was kept at the T_g of the fluorotellurite fiber for 660 ms and then gradually cooled to the room temperature by adjusting the power of the CO_2 laser (like an annealing process) to enhance the strength of the fusion splicing point. The microscope photo of the fusion splicing point was shown in the inset of Fig. 2(a). The silica fiber end was wrapped by the fluorotellurite fiber. The wrapping enhanced the splicing strength of fluorotellurite and silica fibers. A continuous-wave fiber laser operating at 2000 nm was used to measure the transmission loss of the silica-fluorotellurite fiber fusion splicing joint. An overall output power transmission rate of the fluorotellurite fiber with respect to the output power of the test light source is 68 %, corresponding to a loss of ~1.65 dB. Considering the transmission loss caused by mode-field mismatch (0.36 dB), and the intrinsic attenuation of the fiber (1.7 dB/m at 2000 nm), the loss of the

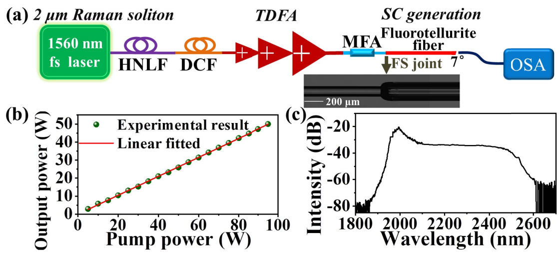

Fig. 2. (a) Experimental setup for all-fiber MIR-SC light source. Inset: Microscope photograph of the fusion splicing point. (b) Power characteristics of the 1.93∼2.5 μm SC laser. (c) Output spectrum of the 1.93∼2.5 μm SC laser. (HNLF, high nonlinear optical fiber; DCF, dispersion compensation fiber; MFA, mode field adapter).

silica-fluorotellurite fiber joint was ∼0.34 dB at 2000 nm. Such a low fusion splicing loss was necessary for constructing all-fiber MIR-SC light source based on fluorotellurite fibers.

Figure 2(a) shows the experimental setup for all-fiber MIR-SC light source. The pump source was a high-power 1.93∼2.5 μm SC laser output from a Tm^{3+}-doped fiber amplifier (TDFA) seeded with a 2000 nm Raman soliton fiber laser (repetition rate: 50 MHz). Figure 2(b) shows the power characteristics of the 1.93∼2.5 μm SC laser. The maximum available average output power was about 50 W and the corresponding conversion efficiency was about 53%. The output spectrum of the 1.93∼2.5 μm SC laser was shown in Fig. 2(c). The 10-dB spectral bandwidth was about 599 nm excluding the pump light, and the corresponding spectral range was from 1938 to 2537 nm. The spectral broadening on the red side was mainly caused by the generation of Raman soliton self-frequency shift. The output fiber of the 1.93∼2.5 μm SC laser was passive double cladding silica fiber with a core/cladding diameter of 10/130 μm and an effective core/cladding NA of 0.15/0.46. The silica fiber was connected to the above fluorotellurite fiber with a length of ∼0.56 m by direct fusion splicing. To prevent reflections in the system, the output end of the fluorotellurite fiber was angle-cleaved. The output signals were monitored by using an optical spectrum analyzer with a measurement range of 600-1700, 1200-2400, or 1900-5500 nm (Yokogawa). The output power of the all-fiber MIR-SC light source was measured by using a power meter.

Figure 3(a) shows measured SC spectrum evolution under different output powers from the above fluorotellurite fiber. With increasing the launched average pump power to 5 W, the average output power of the generated SC light was gradually increased to 3.3 W, large spectral broadening around the pump light occurred and an emission peak at 1677 nm appeared. Since the operating wavelength of the pump light was located in the anomalous dispersion region of the above fluorotellurite fiber, large spectral broadening for a launched average pump power of ≥5 W (corresponding to an average output power of ≥3.3 W) was caused by self-phase modulation, higher-order soliton compression, soliton fission, Raman soliton self-frequency shift, and the generation of blueshifted dispersive waves. The spectral broadening on the blue side was mainly caused by the generation of blueshifted dispersive waves. Raman soliton self-frequency shift contributed the spectral broadening on the red side. As the launched average pump

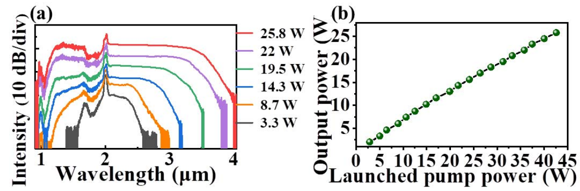

Fig. 3. (a) SC spectrum evolution under different output powers from the fluorotellurite fiber. (b) Dependence of the average power output from fluorotellurite fiber on the launched pump power.

power was increased to 42.6 W, the average output power of the generated SC light was about 25.8 W, the short wavelength edge of SC spectrum was expanded to 0.93 μm, and the long wavelength edge was expanded to 3.99 μm. That is to say, a 25.8 W SC light source with a spectral range from 0.93 to 3.99 μm was obtained by using fluorotellurite fibers we developed. The 10 dB bandwidth of the generated SC light was 2400 nm, and the corresponding spectral range was from 1158 to 3558 nm. Figure 3(b) shows the dependence of the average output power of the generated SC light in the fluorotellurite fiber on the launched average power of the pump laser. With increasing the launched average pump power to 42.6 W, the average output power of the generated SC light was gradually increased to 25.8 W, and the corresponding optical-to-optical conversion efficiency was about 60.6%. The fluorotellurite fiber used for SC generation had a bend radius of about 30 cm. There are no obvious changes on the output spectra or power was observed with slightly adjusting the bend radius of the fiber. A small offset in the splice might result in a narrower output spectrum with a lower output power. Our results showed that high power (>25 W) MIR-SC light sources based on fluorotellurite fibers in all-fiber configuration could be realized by direct fusion splicing of fluorotellurite and silica fibers. To the best of our knowledge, this is the first report of an over 25 W all-fiber MIR-SC light source based on fluorotellurite fibers.

III. Numerical Modeling and Discussions

Moreover, we performed numerical simulations on spectral broadening of the above SC light by solving the generalized Schrödinger equations. In our simulations, the initial pump laser has an operation wavelength of 2000 nm, a pulse width of 2 ps, and a repetition rate of 50 MHz. Two types of nonlinear fibers were used for SC generation. First, a 1.0 m long double cladding single-mode silica fiber was used for SC generation from 1.9 to 2.5 μm. The nonlinear coefficient of the silica fiber we used was about 1 $km^{-1}W^{-1}$, reference [16] shows the Raman response function, the GVD curve was derived from a standard single-mode fiber, reference [17] shows the loss of the silica fiber. By using the generated 1.93 ∼2.5 μm SC light as the pump light, a 0.56 m long fluorotellurite fiber was used as the nonlinear medium for MIR-SC generation. We took the parameters of the above fluorotellurite fiber, including the transmission loss of the fiber, the calculated nonlinear coefficients and the GVD profiles of the LP01, LP11, LP21, LP02, LP31 and LP12 modes in the fiber, and the Raman

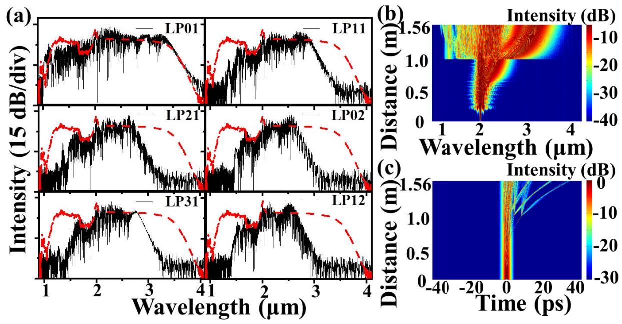

Fig. 4. (a) Simulated SC spectra for LP01, LP11, LP21, LP02, LP31 and LP12 modes, and measured (the red dashed curve) SC spectra output from the fluorotellurite fiber for a launched average pump power of ~42.6 W. (b), (c) Simulated spectral and temporal evolution of SC generation in concatenated 1 m double cladding silica fiber and 0.56 m fluorotellurite fiber (LP01 mode) for a launched average pump power of ~42.6 W.

response function derived from the Raman gain spectrum of fluorotellurite glass [14].

Figure 4(a) shows the simulated SC spectra for LP01, LP11, LP21, LP02, LP31 and LP12 modes, and measured (the red dashed curve) SC spectra output from the fluorotellurite fiber for a launched average pump power of ~42.6 W. For LP01 mode, the simulated SC spectrum agreed with the measured one. However, the simulated SC spectra for LP01, LP11, LP21, LP02, LP31 and LP12 modes did not agree with the measure one, both the long and short wavelength edges of the simulated spectra were shorter than those of the measured one. SC generation in higher order modes (including LP41, LP22, LP03, LP51, LP32, LP13, LP23, LP04, LP33 and LP14 modes) was also calculated and much narrower bandwidths were obtained. The above results indicated that the measured SC light was mainly generated by the excitation of the LP01 in the fiber. In the future, we will analyze the mode characteristics of the measured SC light and improve its performance by optimizing the parameters of the fluorotellurite glass fiber. Figure 4(b) shows the simulated spectral evolution of SC generation for a launched average pump power of ~42.6 W. As the pump light propagated inside the fiber segment from 0 to 1 m (the silica fiber), the spectral broadening was caused by self-phase modulation, modulation instability, higher-order soliton compression, soliton fission, and Raman soliton self-frequency shift. For the pump light propagation inside the fiber segment from 1 to 1.56 m (the fluorotellurite fiber, LP01 mode), large spectral broadening occurred owing to Raman soliton self-frequency shift, and the generation of blueshifted dispersive waves. The spectral broadening on the blue side was mainly caused by the generation of blueshifted dispersive waves, and Raman soliton self-frequency shift contributed to the spectral broadening on the red side. The simulated temporal evolution of SC generation for a launched average pump power of ~42.6 W was shown in Fig. 4(c), which confirmed the above interpretation.

In addition, the long time stability of the 25.8 W all-fiber MIR-SC light source based on fluorotellurite fibers was investigated. No obvious damage was observed on the end surface of the fluorotellurite fiber and the silica-fluorotellurite fiber joint after the 25.8 W all-fiber MIR-SC light source was operating for over 10 h. The maximum output power and the spectral bandwidth of the all-fiber MIR-SC laser sources obtained in the above experiments was mainly limited by the average power of the 1.93–2.5 μm SC laser which could be realized by us currently.

IV. Summary

In summary, we demonstrated a 25.8 W MIR-SC light source based on fluorotellurite fibers in all-fiber configuration. Direct fusion splicing was used to realize the connection between fluorotellurite fibers and silica fibers, leading to the formation of the compact all-fiber structure. Our results paved the way to apply high power MIR-SC light sources based on fluorotellurite fibers for real applications.

References

[1] K. Ke, C. Xia, M. N. Islam, M. J. Welsh, and M. J. Freeman, "Mid-infrared absorption spectroscopy and differential damage *in vitro* between lipids and proteins by an all-fiber-integrated supercontinuum laser," *Opt. Exp.*, vol. 17, no. 15, pp. 12627–12640, May 2009.

[2] S. Dupont, C. Petersen, J. Thogersen, C. Agger, O. Bang, and S. R. Keiding, "IR microscopy utilizing intense supercontinuum light source," *Opt. Exp.*, vol. 20, no. 5, pp. 4887–4892, Feb. 2012.

[3] C. R. Petersen *et al.*, "Mid-infrared multispectral tissue imaging using a chalcogenide fiber supercontinuum source," *Opt. Lett.*, vol. 43, no. 5, pp. 999–1002, Mar. 2018.

[4] C. R. Petersen, P. M. Moselund, L. Huot, L. Hooper, and O. Bang, "Towards a table-top synchrotron based on supercontinuum generation," *Infr. Phys. Technol.*, vol. 91, no. 8, pp. 182–186, Jun. 2018.

[5] N. M. Israelsen *et al.*, "Real-time high-resolution mid-infrared optical coherence tomography," *Light, Sci. Appl.*, vol. 8, no. 1, pp. 114–126, Dec. 2019.

[6] C. Xia *et al.*, "10.5 W time-averaged power mid-IR supercontinuum generation extending beyond 4 μm with direct pulse pattern modulation," *IEEE J. Sel. Top. Quantum Electron*, vol. 15, no. 2, pp. 422–433, Apr. 2009.

[7] W. Yang, B. Zhang, G. Xue, K. Yin, and J. Hou, "Thirteen watt all-fiber mid-infrared supercontinuum generation in a single mode ZBLAN fiber pumped by a 2 μm MOPA system," *Opt. Lett.*, vol. 39, no. 7, pp. 1849–1852, Mar. 2014.

[8] K. Liu, J. Liu, H. Shi, F. Tan, and P. Wang, "High power mid-infrared supercontinuum generation in a single-mode ZBLAN fiber with up to 21.8 W average output power," *Opt. Exp.*, vol. 22, no. 20, pp. 24384–24391, Sep. 2014.

[9] L. Yang, Y. Li, B. Zhang, T. Wu, Y. Zhao, and J. Hou, "30-W supercontinuum generation based on ZBLAN fiber in an all-fiber configuration," *Photon. Res.*, vol. 7, no. 9, pp. 1061–1065, Sep. 2019.

[10] L. Yang, B. Zhang, X. He, K. Deng, S. Liu, and J. Hou, "20.6 W mid-infrared supercontinuum generation in ZBLAN fiber with spectrum of 1.9–4.3 μm," *J. Lightwave. Technol.*, vol. 38, no. 38, pp. 5122–5127, Jun. 15, 2020.

[11] T. Wu *et al.*, "Ultra-efficient, 10-watt-level mid-infrared supercontinuum generation in fluoroindate fiber," *Opt. Lett.*, vol. 44, no. 9, pp. 2378–2381, May 2019.

[12] G. H. Frischat, B. Hueber, and B. Ramdohr, "Chemical stability of ZrF_4- and AlF_3-based heavy metal fluoride glasses in water," *J. Non-Crystalline Solids*, vol. 284, nos. 1–3, pp. 105–109, May 2001.

[13] C. Yao *et al.*, "High-power mid-infrared supercontinuum laser source using fluorotellurite fiber," *Optica*, vol. 5, no. 10, pp. 1264–1270, Oct. 2018.

[14] Z. Li *et al.*, "22.7 W mid-infrared supercontinuum generation in fluorotellurite fibers," *Opt. Lett.*, vol. 45, no. 7, pp. 1882–1885, Apr. 2020.

[15] Z. X. Jia *et al.*, "Supercontinuum generation covering the entire 0.4–5 μm transmission window in a tapered ultra-high numerical aperture all-solid fluorotellurite fiber," *Laser Phys. Lett.*, vol. 15, no. 2, Jan. 2018, Art. no. 025102.

[16] P. V. Mamyshev and S. V. Chernikov, "Ultrashort-pulse propagation in optical fibers," *Opt. Lett.*, vol. 15, no. 19, pp. 1076–1078, Oct. 1990.

[17] T. Li, "Optical fiber communications: Fiber fabrication," *Opt. Laser Technol.*, vol. 17, no. 5, p. 274, Oct. 1985.